# Globular clusters with multiple stellar populations. Where they came from?

M.E. Sharina (SAO RAS), A. Y. Kniazev (SAAO, SAI MSU), V. V. Shimansky (KFU)

*We found a group of old Galactic globular clusters with very similar medium-resolution spectra:* ***NGC6254, NGC7089, NGC5286, NGC6752 and NGC1904****.The long-slit spectra were taken from the library of Schiavon et al. (2005) and obtained with the CARELEC spectrograph of the 1.93-m telescope in the Haute Provence Observatory. We analyzed the spectra using our method of population synthesis using stellar atmospheres models (Sharina et al. 2013, 2014; Khamidullina et al. 2014).Our method allows to derive age, [Fe/H], Y and abundances of 8 chemical elements using medium-resolution integrated-light spectra of globular clusters. All the sample Galactic GCs have extended blue horizontal branches. Multiple stellar population were discovered in the literature in several of them. We study whether their distribution is correlated with the position of Galactic satellites and streams.*

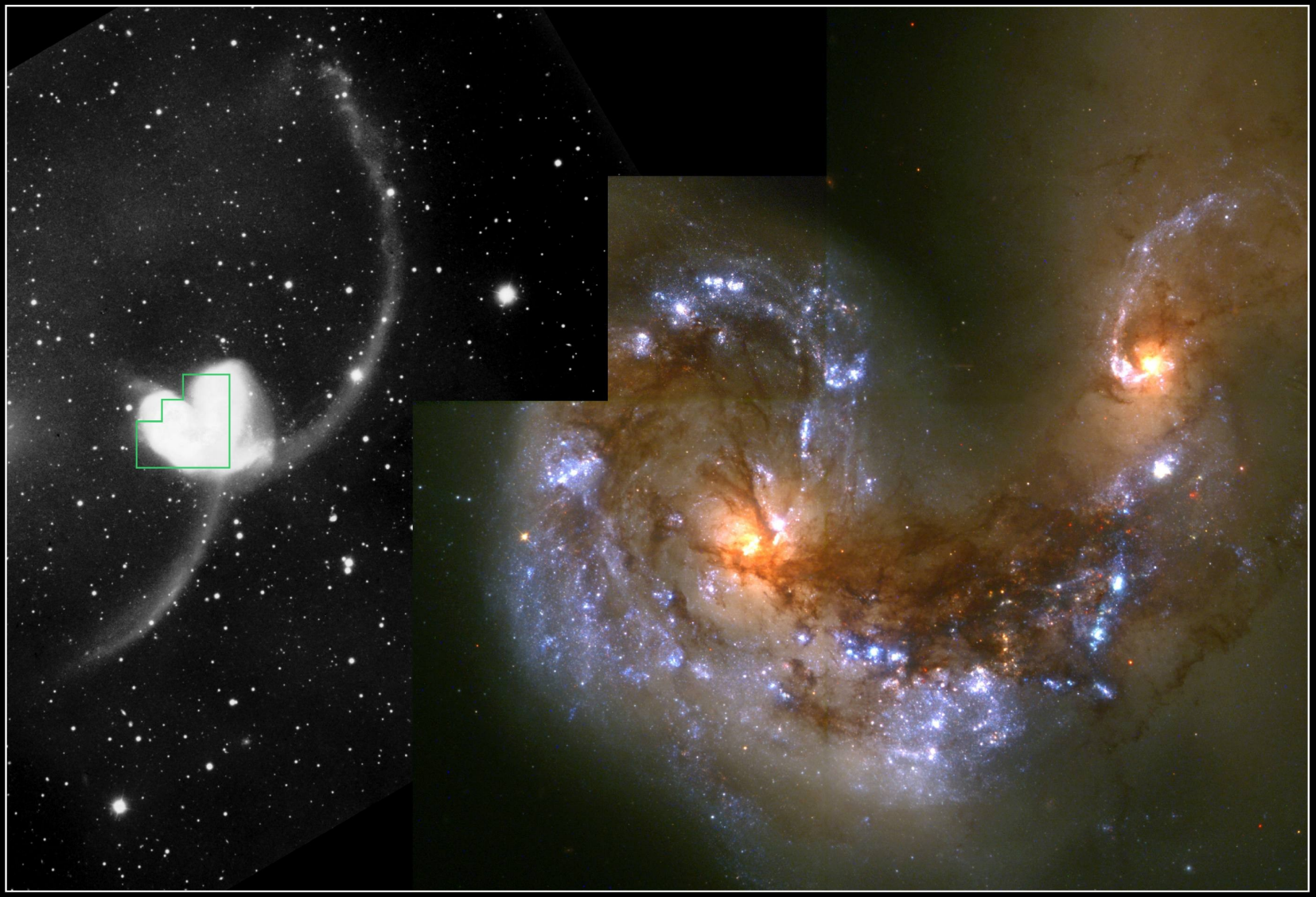

**Colliding Galaxies NGC 4038 and NGC 4039**

Hubble Space Telescope • Wide Field Planetary Camera 2

PRC97-34a • ST ScI OPO • October 21, 1997 • B. Whitmore (ST ScI) and NASA

**Dist. = 13.3 Mpc**

**V= 10.3 mag.**

**Size=5.2' x 3.1'**
**3.1' x 1.6'**

**Witmore et al. 1999**

# The Most Luminous cluster

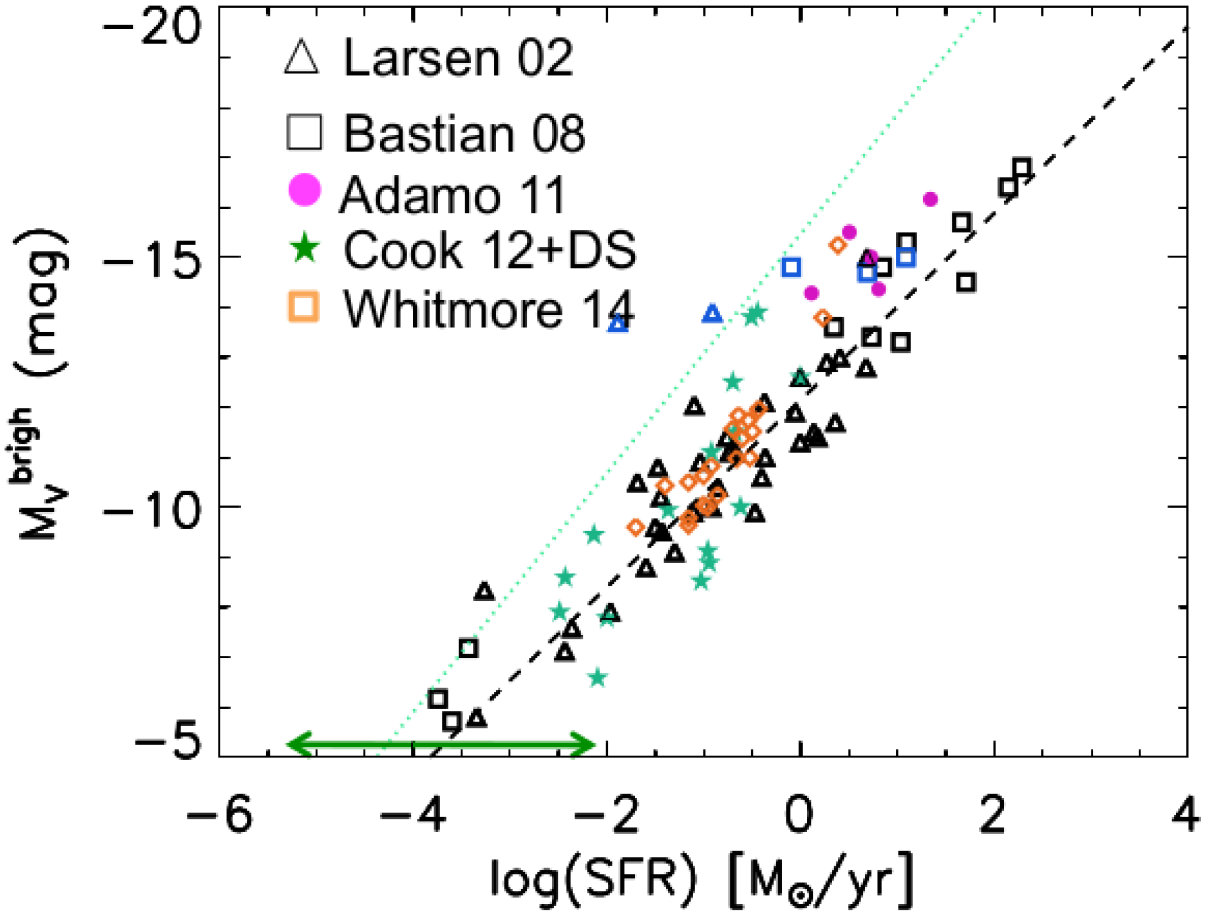


Size of sample effect

↓

galaxies with higher SFR can form more massive clusters → higher probability to sample the high mass cluster bins

Mv (brightest) → is a young cluster and not the most massive

Larsen (2002, 2009), Whitmore (2003), Bastian (2008),Adamo et al (2011), Cook et al. (2012), Whitmore et al (2014)

# Destruction of globular clusters

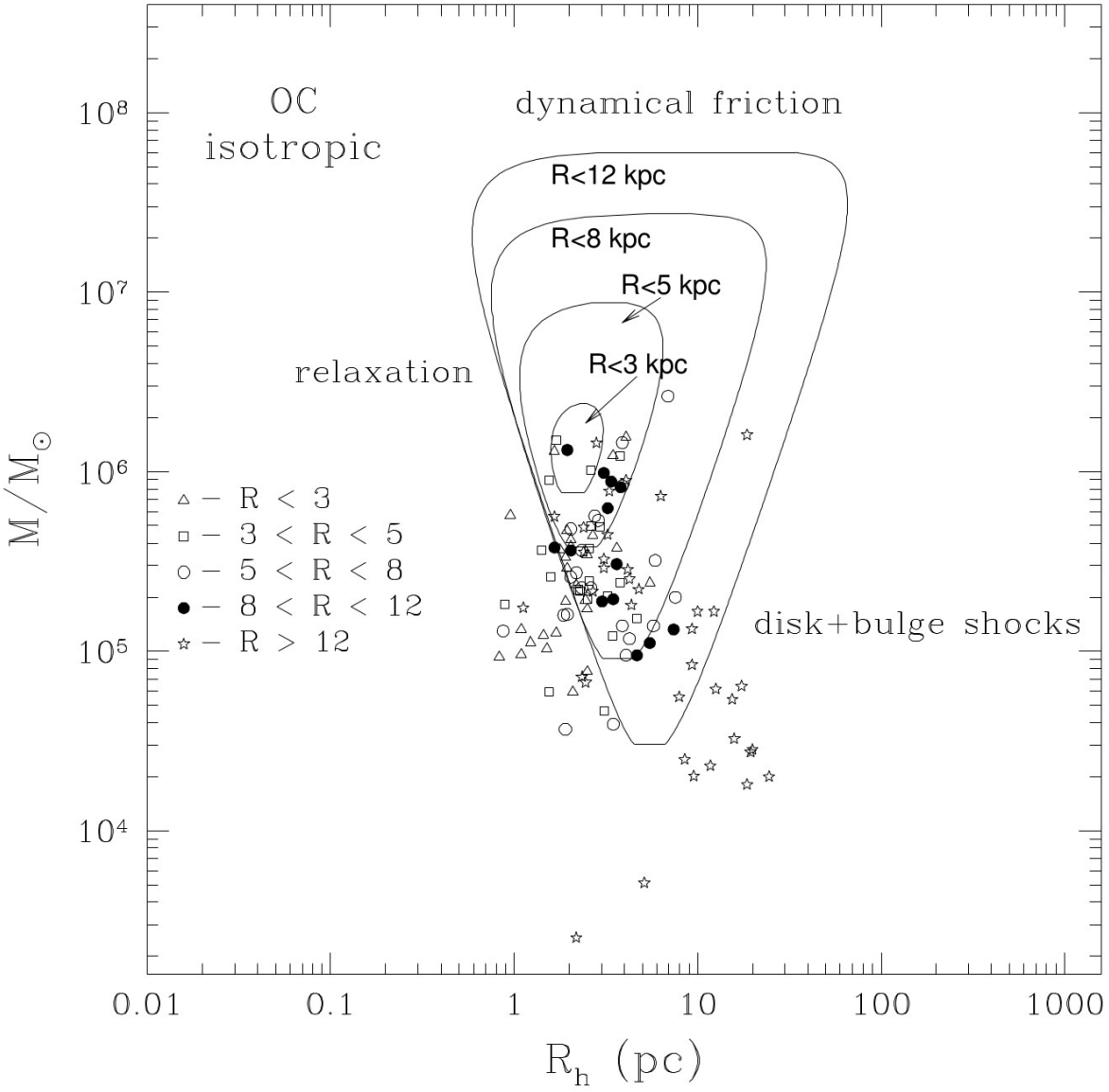


GNEDIN & OSTRIKER, 1997

FIG. 21.—Vital diagram for the Galactic globular clusters. Mass-radius plane is restricted by three destructing processes: relaxation, tidal shocks, and dynamical friction. Galactic model is OC, and the kinematic model is isotropic.

# Globular cluster formation efficiency

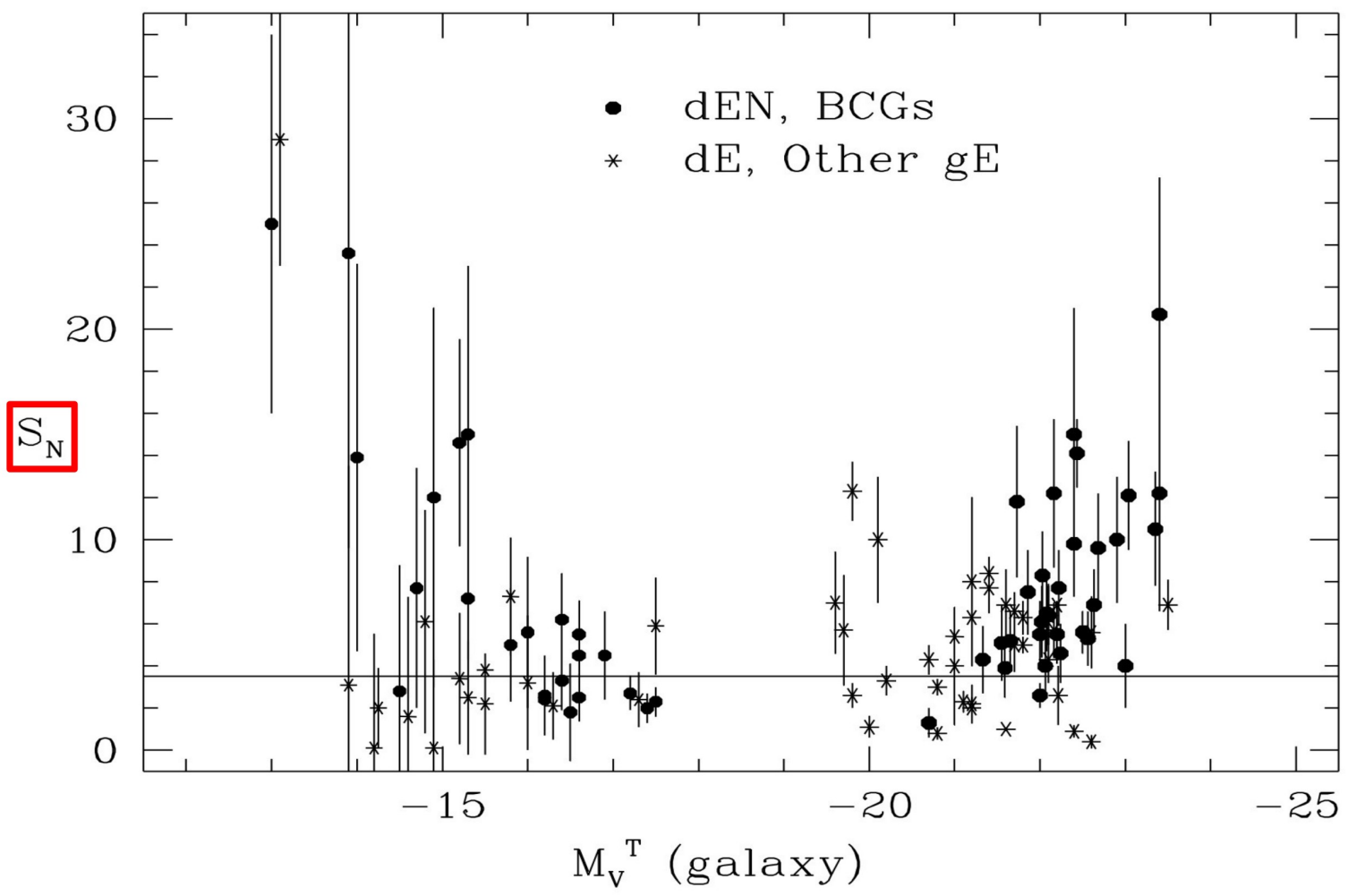


The total population of clusters in a galaxy is usually represented by the *specific frequency* $S_N$, the number of clusters per unit galaxy luminosity (Harris & van den Bergh 1981; Harris 1991):

$$S_N = N_{cl} \cdot 10^{0.4\,(M_V^T + 15)} \qquad (1.47)$$

Harris (2001)

# Luminosity distributions of globular clusters in different galaxies

## Harris W.E. 1998

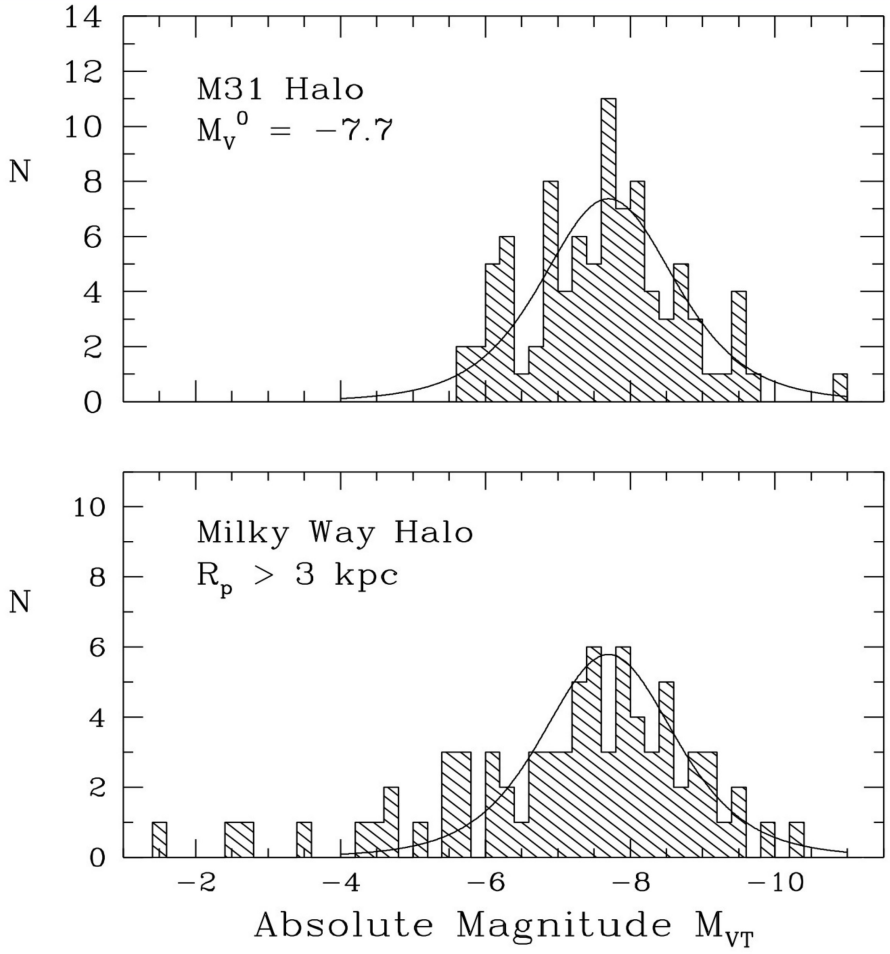


## Jordan et al. 2006, 2007

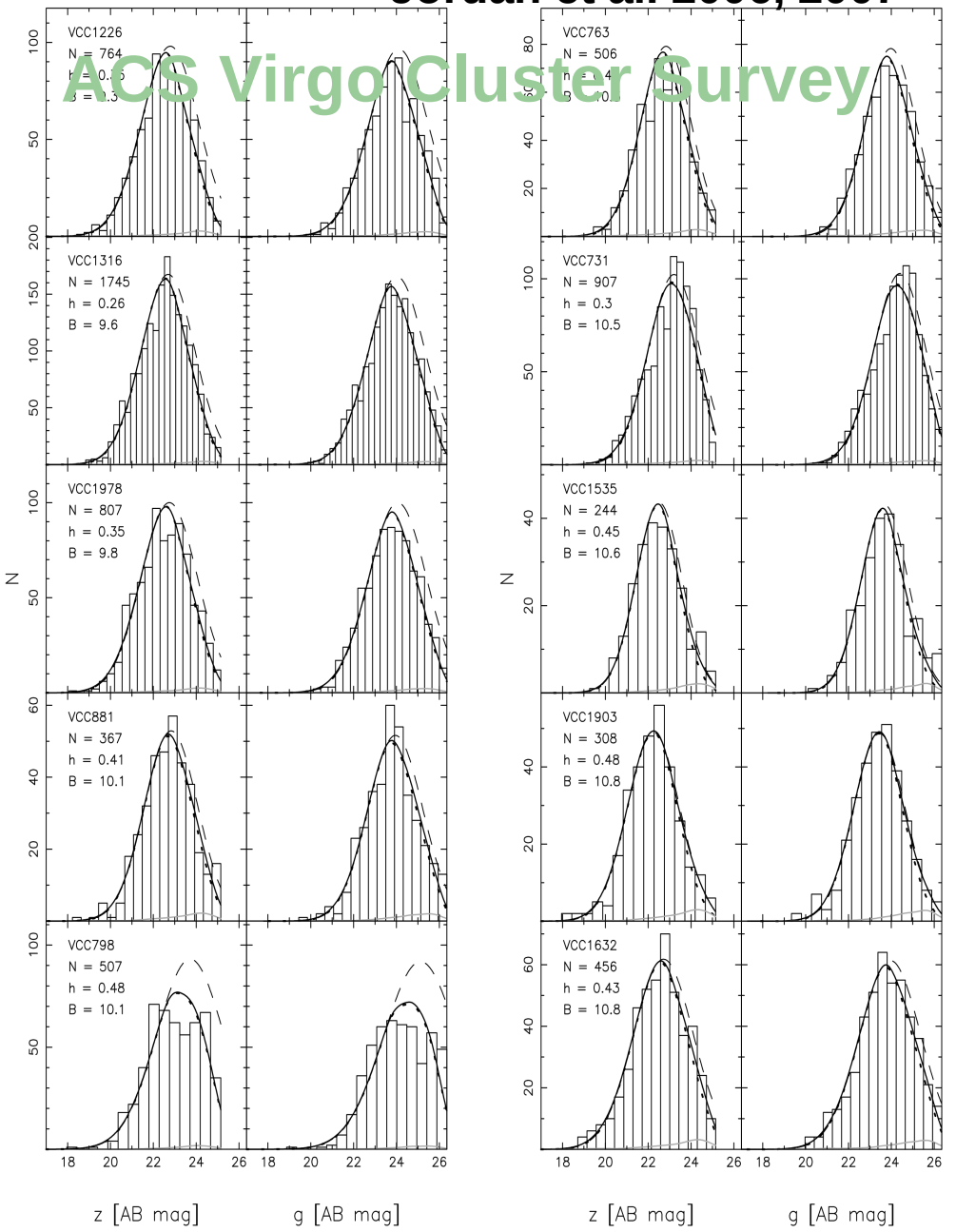


FIG. 4.—Histograms of the GCLFs for our sample galaxies. For each galaxy we present the *z*-band and *g*-band GCLFs side by side. The VCC name and *B* magnitude of the galaxy are indicated in the upper left corner of the left panel, where we also indicate the total number of sources in each histogram and the bin width *h* used to construct the histogram. In addition, we show the best-fit model (*solid black curve*), the intrinsic Gaussian component (*dashed curve*), the Gaussian component multiplied by the expected completeness (*dotted curve*), and a kernel density estimate of the expected contamination in the sample (*solid gray curve*). The solid black curve is the sum of the solid gray and dotted curves. The galaxies are ordered by decreasing apparent *B*-band total luminosity, reading down from the upper left corner. The parameters of the fits are given in Table 2. [*See the electronic edition of the Supplement for a color version of this figure.*]

# Metallicity distribution of globular clusters in different galaxies

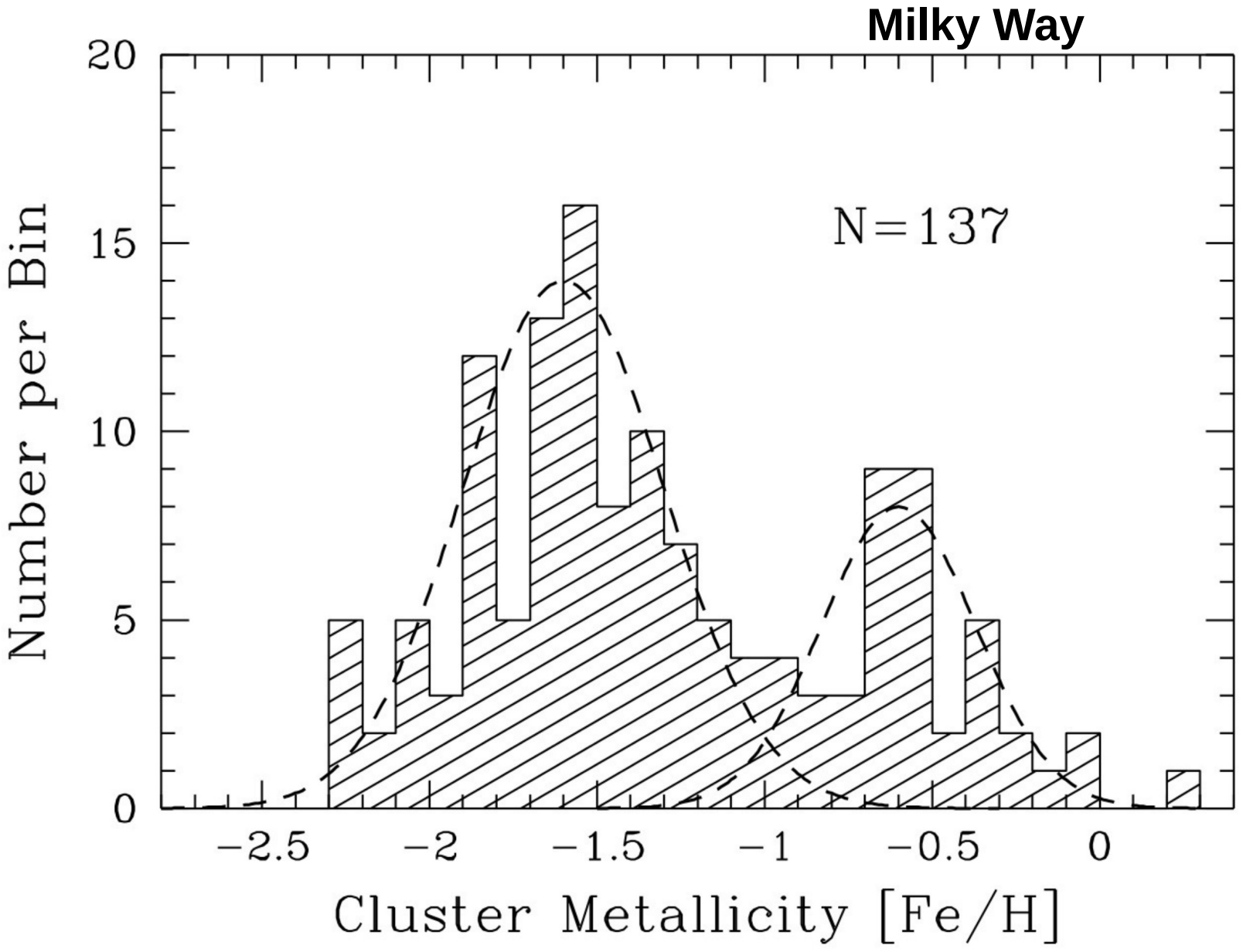


Harris (2001)

# Metallicity distribution of globular clusters, dwarf galaxies and elliptical gs

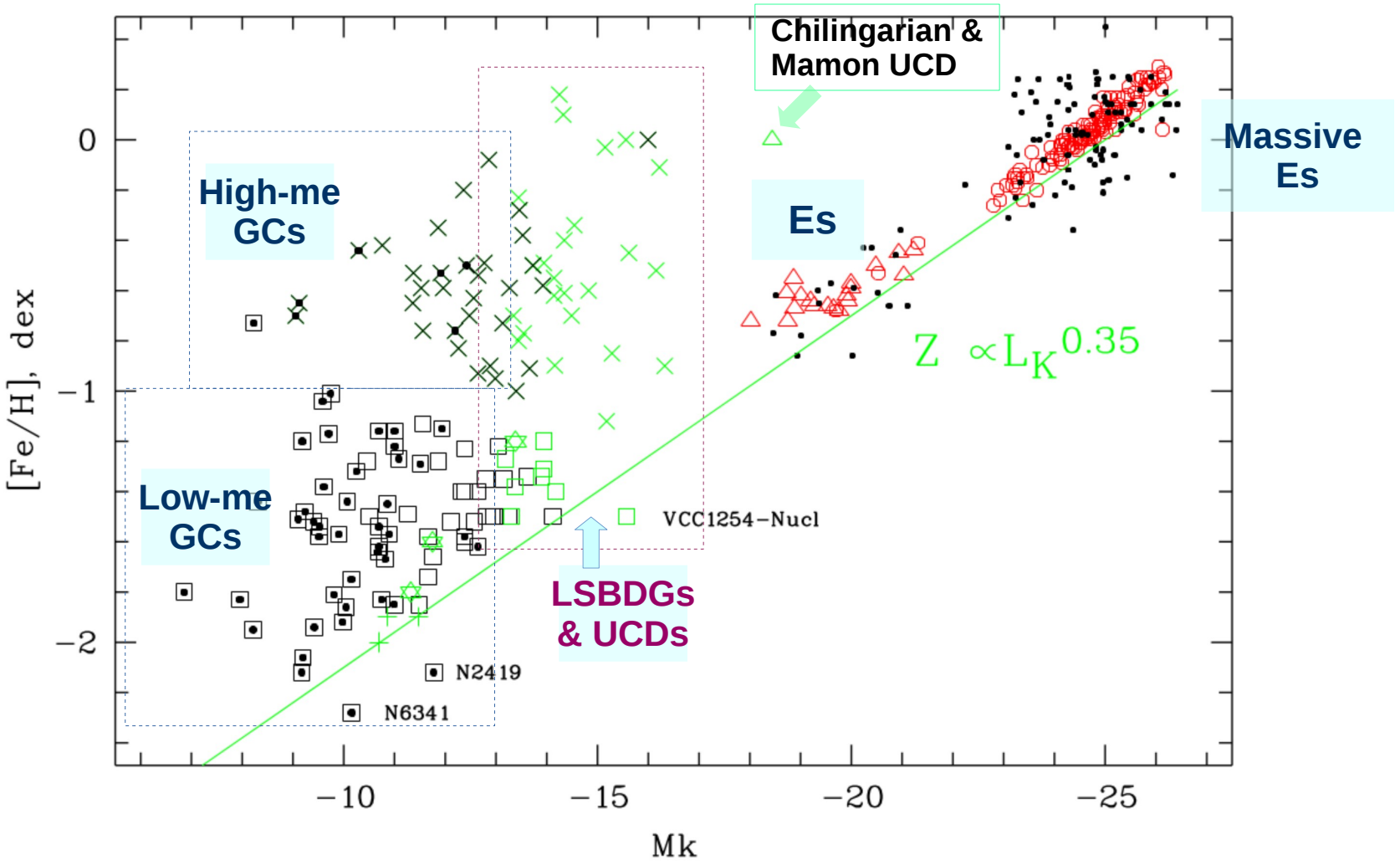


2012ApJ...750...91C

Chattopadhyay, T.; Sharina, M.; Davoust, E.; et al.

Uncovering the Formation of Ultracompact Dwarf Galaxies by Multivariate Statistical Analysis

# Spectroscopic observations of globular clusters in dwarf galaxies

2006AstL...32..185S Sharina, M. E.; Afanasiev, V. L.; Puzia, T. H.
Observations of Lick standard stars with the SCORPIO multislit unit at the SAO 6-m telescop

2006MNRAS.372.1259S Sharina, M. E.; Afanasiev, V. L.; Puzia, T. H.
Ages, metallicities and [alpha/Fe] ratios of globular clusters in NGC 147, 185 and 205

2007AstBu..62..209S Sharina, M. E.; Puzia, T. H.; Krylatyh, A. S.
A globular cluster in the dwarf galaxy Sextans B

2008ApJ...674..909P Puzia, Thomas H.; Sharina, Margarita E.
VLT Spectroscopy of Globular Clusters in Low Surface Brightness Dwarf Galaxies

2009A&A...497...65S Sharina, M.; Davoust, E.
Globular cluster content and evolutionary history of NGC 147

2010MNRAS.405..839S Sharina, M. ; Chandar, R.; Puzia, T.; Goudfrooij, P.; Davoust, E.
SAO RAS 6-m telescope spectroscopic observations of globular clusters in nearby galaxies

2011EAS....48..237S Sharina, M. ; Chandar, R.; Puzia, T. ; Goudfrooij, P.; Davoust, E.
Observational Properties of Globular Clusters in Dwarf Galaxies

2013ARep...57..410S Sharina, M. E.; Shimansky, V. V.; Davoust, E.
Modeling and analysis of the spectrum of the globular cluster NGC 2419

2014A&A...570A..48S Sharina, M.; Donzelli, C.; Davoust, E.; Shimansky, V.; Charbonnel, C.;
Gemini spectroscopy of the outer disk star cluster BH176

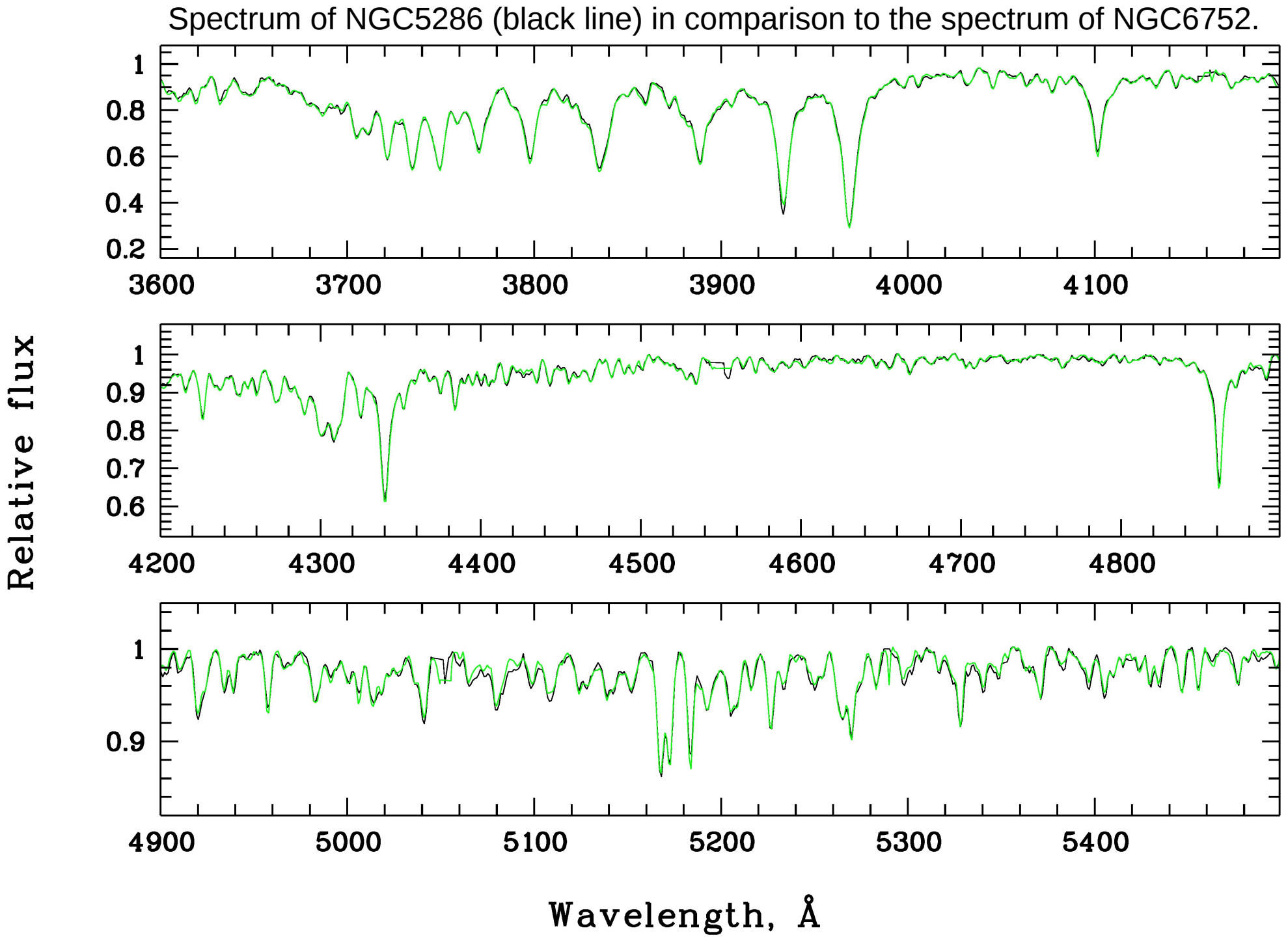
Spectrum of NGC5286 (black line) in comparison to the spectrum of NGC6752.
Relative flux
1
0.8
0.6
0.4
0.2
3600
3700
3800
3900
4000
4100
1
0.9
0.8
0.7
0.6
4200
4300
4400
4500
4600
4700
4800
1
0.9
4900
5000
5100
5200
5300
5400
Wavelength, Å

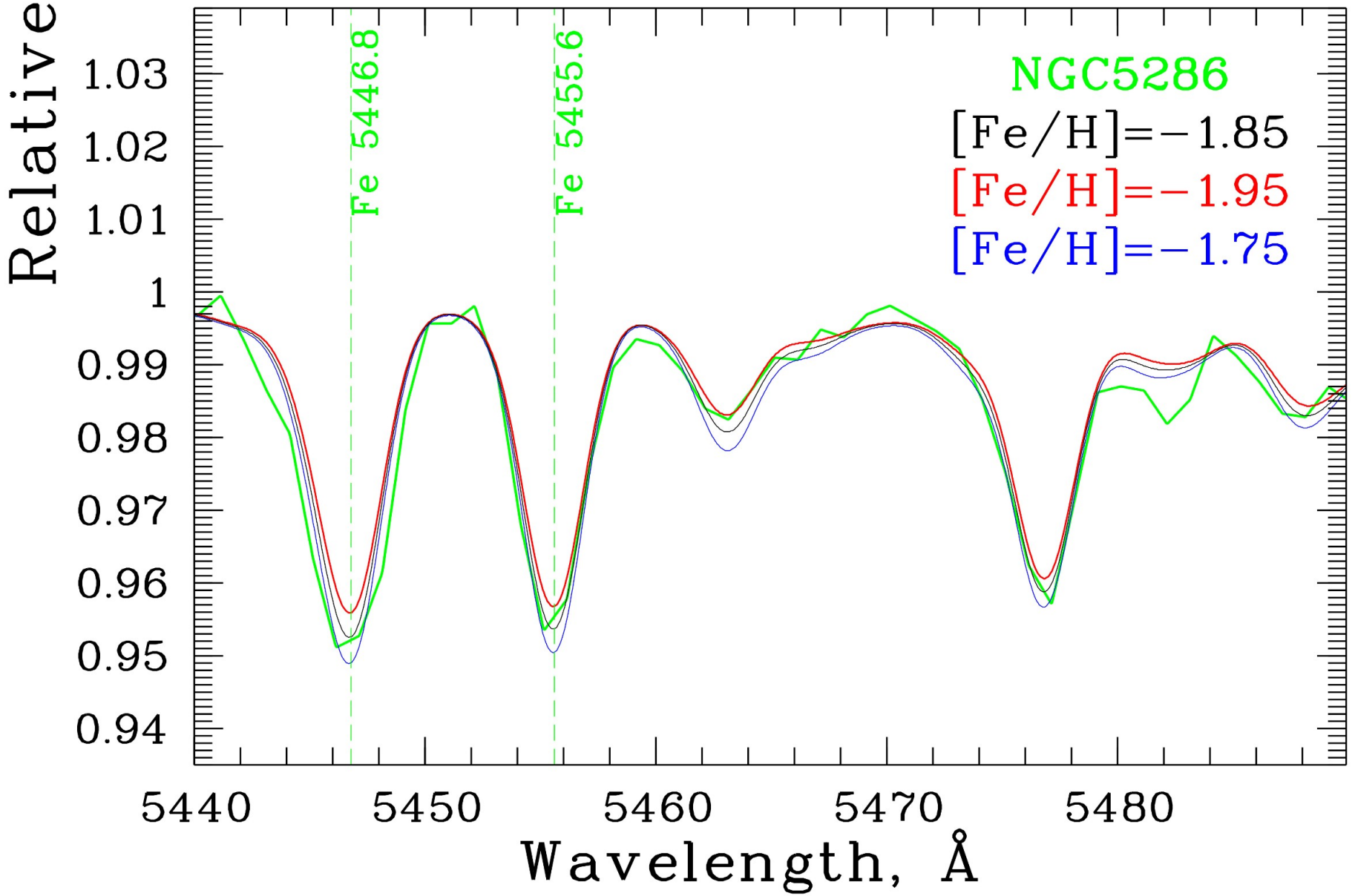
Relative
1.03
1.02
1.01
1
0.99
0.98
0.97
0.96
0.95
0.94
Fe 5446.8
Fe 5455.6
NGC5286
[Fe/H]=−1.85
[Fe/H]=−1.95
[Fe/H]=−1.75
5440
5450
5460
5470
5480
Wavelength, Å

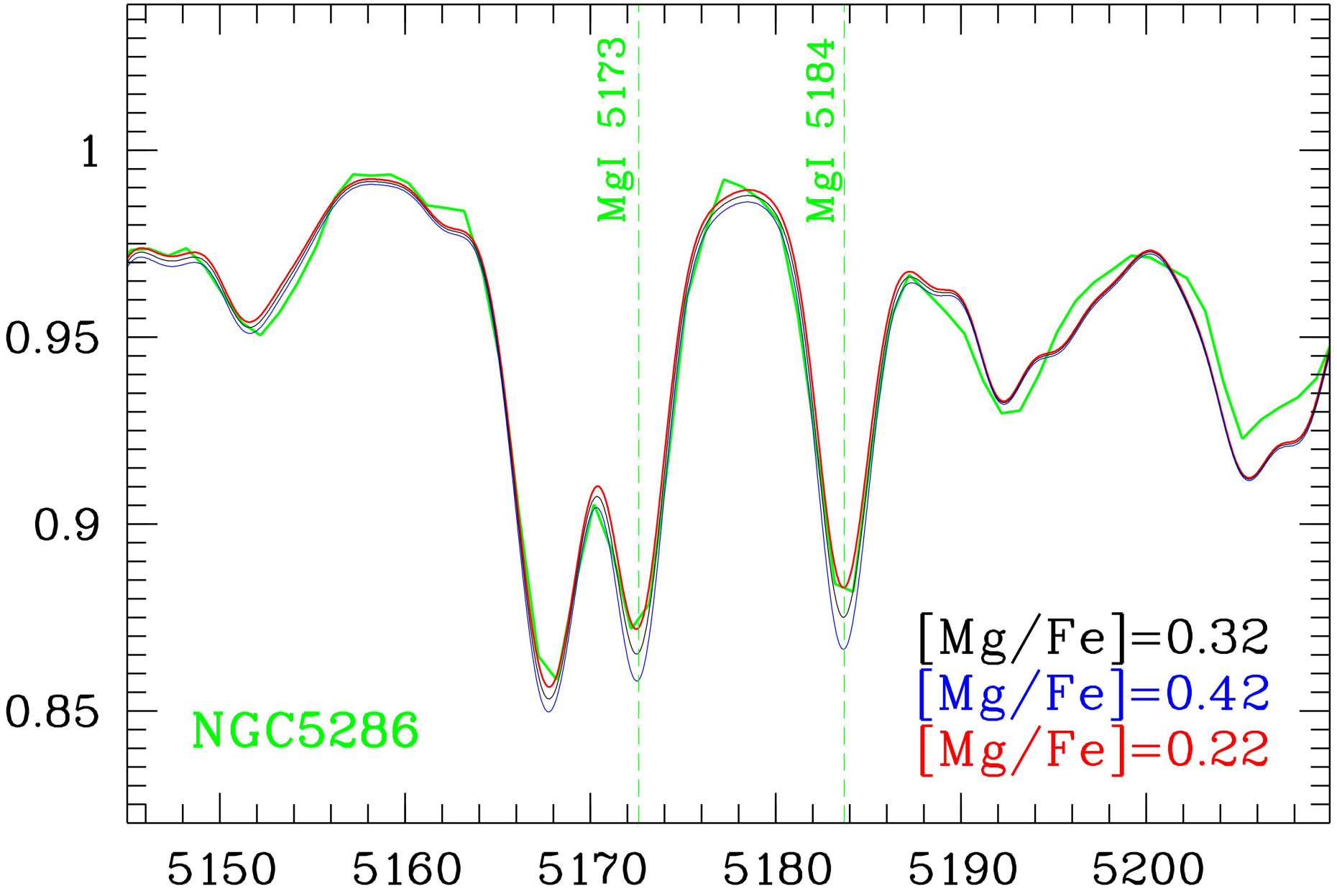
MgI 5173
MgI 5184
1
0.95
0.9
0.85
NGC5286
[Mg/Fe]=0.32
[Mg/Fe]=0.42
[Mg/Fe]=0.22
5150
5160
5170
5180
5190
5200

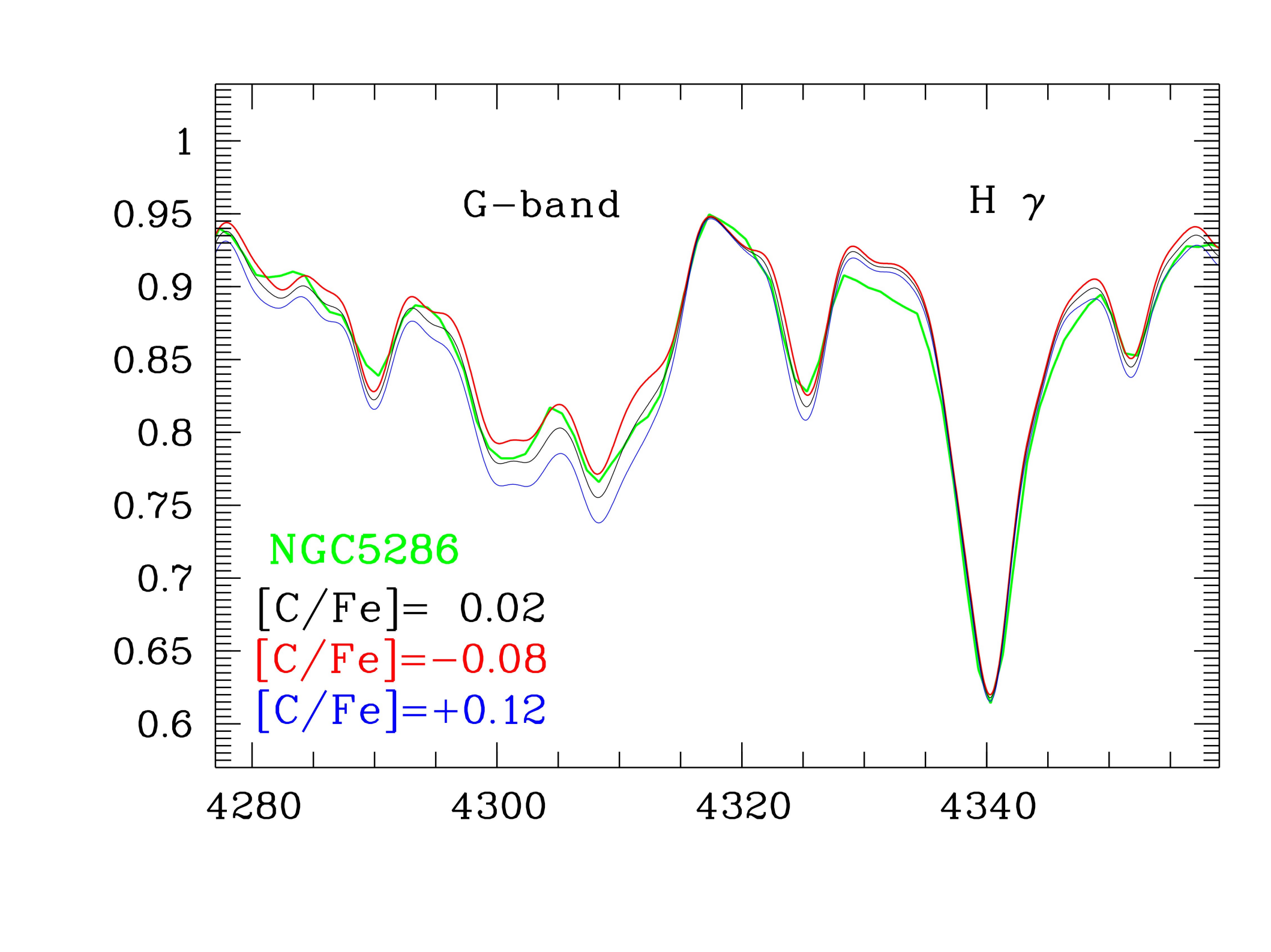
G−band
H γ
NGC5286
[C/Fe]= 0.02
[C/Fe]=−0.08
[C/Fe]=+0.12
1
0.95
0.9
0.85
0.8
0.75
0.7
0.65
0.6
4280
4300
4320
4340

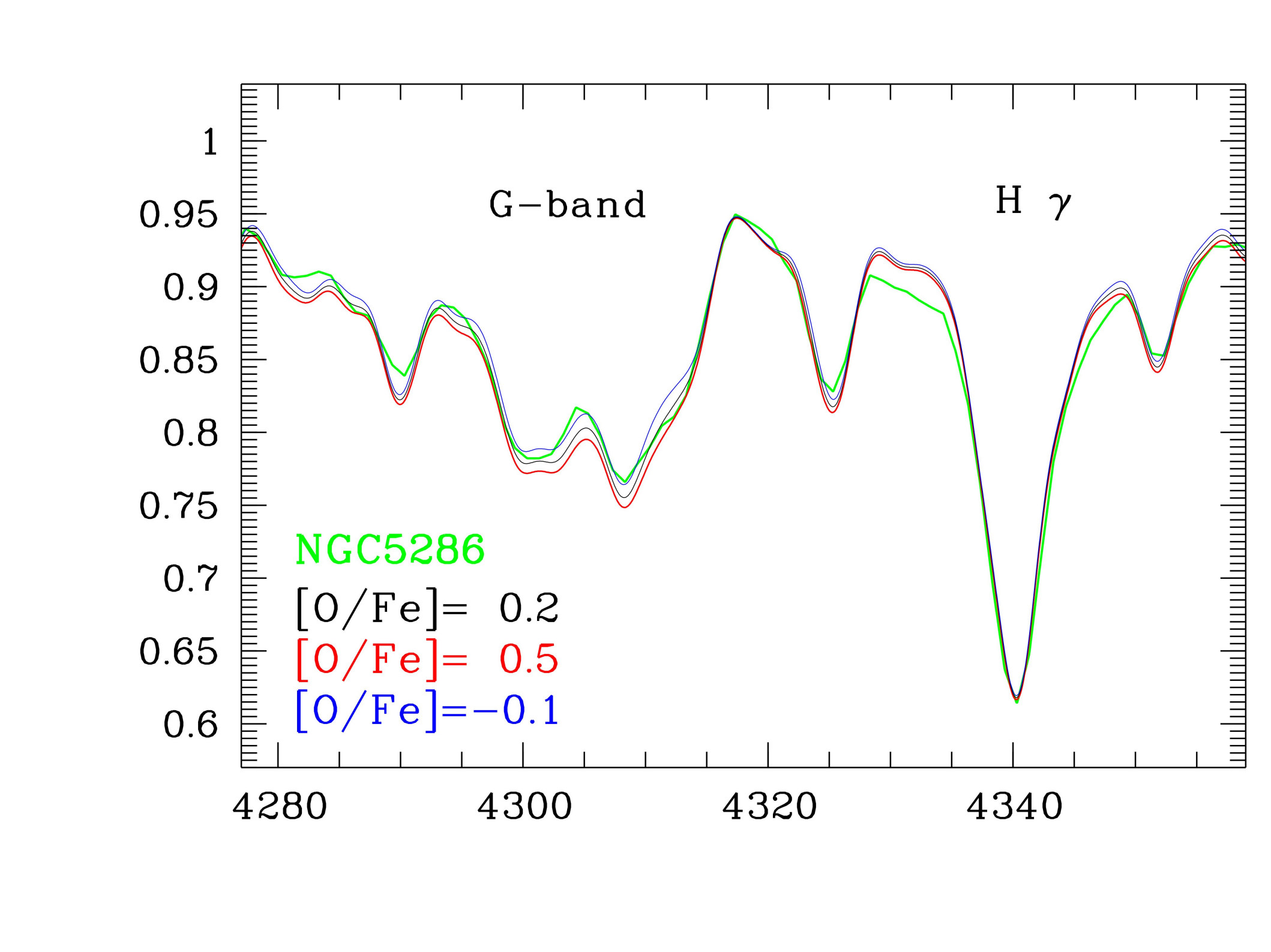
G−band
H γ
NGC5286
[O/Fe]= 0.2
[O/Fe]= 0.5
[O/Fe]=−0.1
1
0.95
0.9
0.85
0.8
0.75
0.7
0.65
0.6
4280
4300
4320
4340

**Our method (Sharina et  al. 2013, 2014 and Khamidullina et al. , 2014)**

We use integrated-light medium-resolution spectra (FWHM~3--5AA) in the spectral range 3900--5500 AA of globular clusters and model stellar atmospheres to carry out population synthesis and to derive the chemical composition and age of the clusters using full-spectrum fitting. The analysis of medium-resolution spectra permits to use only blends of lines and molecular bands, but not individual lines of chemical elements. Thus, to reach reliable results one has to consider high signal-to-noise spectra (S/N >=100) containing several absorption line features of the element in a wide spectral range. The synthetic blanketed spectra of stars are computed according to their masses, radii, Teff, surface gravities and metallicities by interpolating the model grid of Castelli & Kurucz (2003). The stellar parameters are set by models of stellar evolution by Bertelli et al. (2009), because these models contain the Horizontal branch and Asymptotic branch stages of evolution and a wide range of model parameters (metallicity, alpha-element ratio, age and helium content). The computed synthetic blanketed spectra of stars are summed according to the Chabrier mass function (Chabrier, 2005).

ISSN 1063-7729, Astronomy Reports, 2013, Vol. 57, No. 6, pp. 410–422. © Pleiades Publishing, Ltd., 2013.
Original Russian Text © M.E. Sharina, V.V. Shimansky, E. Davoust, 2013, published in Astronomicheskii Zhurnal, 2013, Vol. 90, No. 6, pp. 453–465.

# Modeling and Analysis of the Spectrum of the Globular Cluster NGC 2419

M. E. Sharina[1*], V. V. Shimansky[2], and E. Davoust[3]

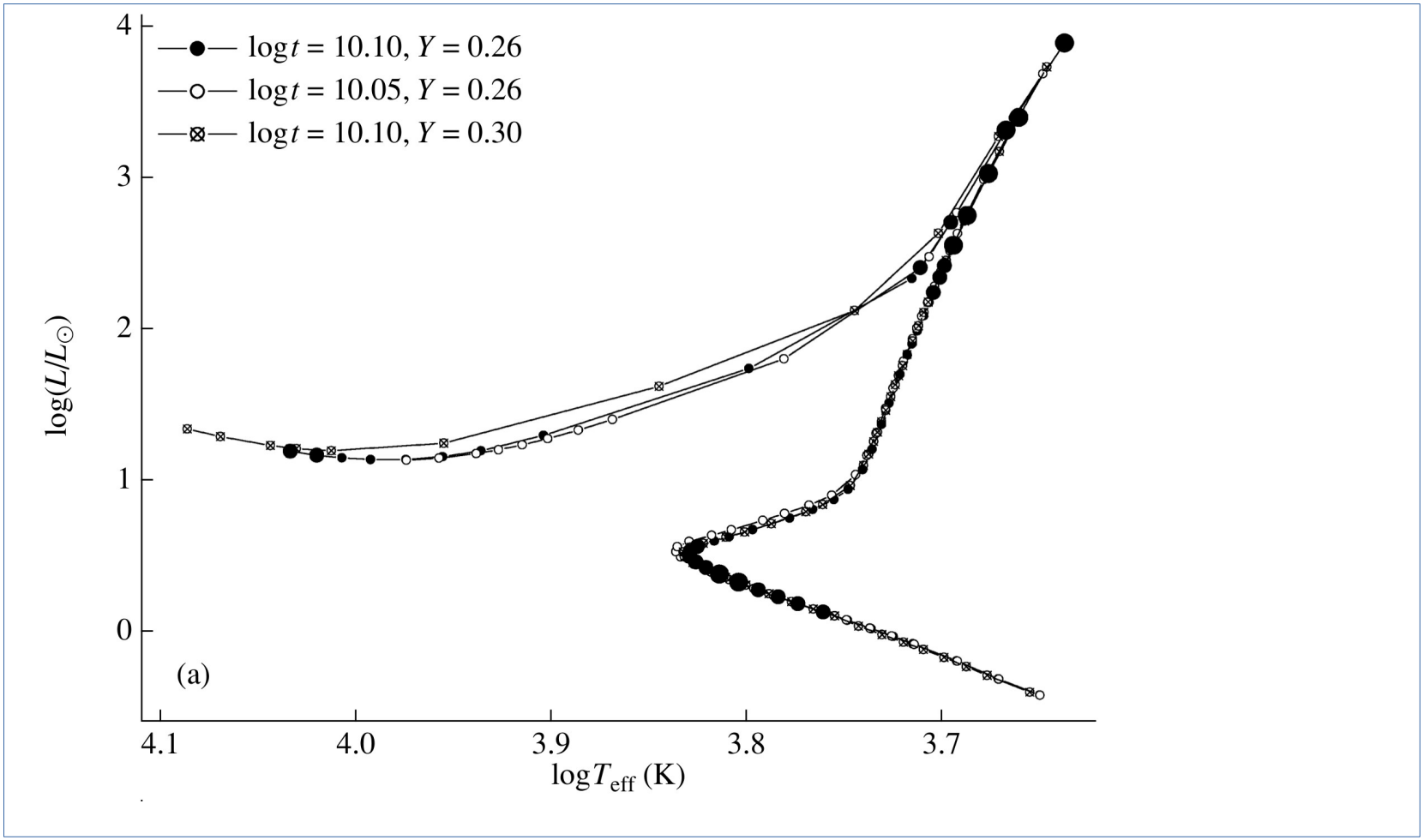


Isochrones from Bertelli et al.(2009). The circles of different size denote points with the contribution to the integraated ligh of NGC2419 are : <1%, 1-3% and >3%.

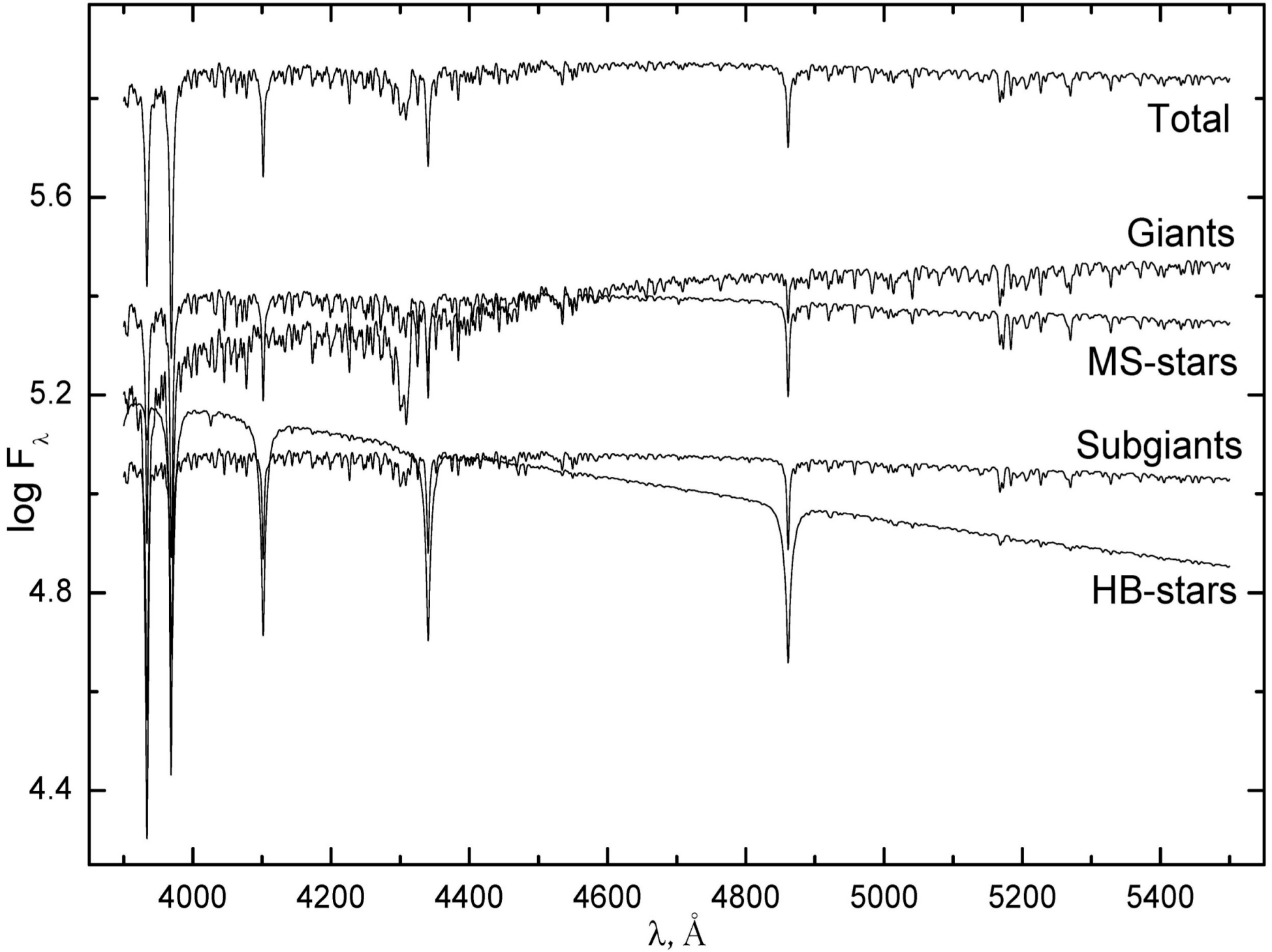
Total
Giants
MS-stars
Subgiants
HB-stars
log F λ
5.6
5.2
4.8
4.4
4000
4200
4400
4600
4800
5000
5200
5400
λ, Å

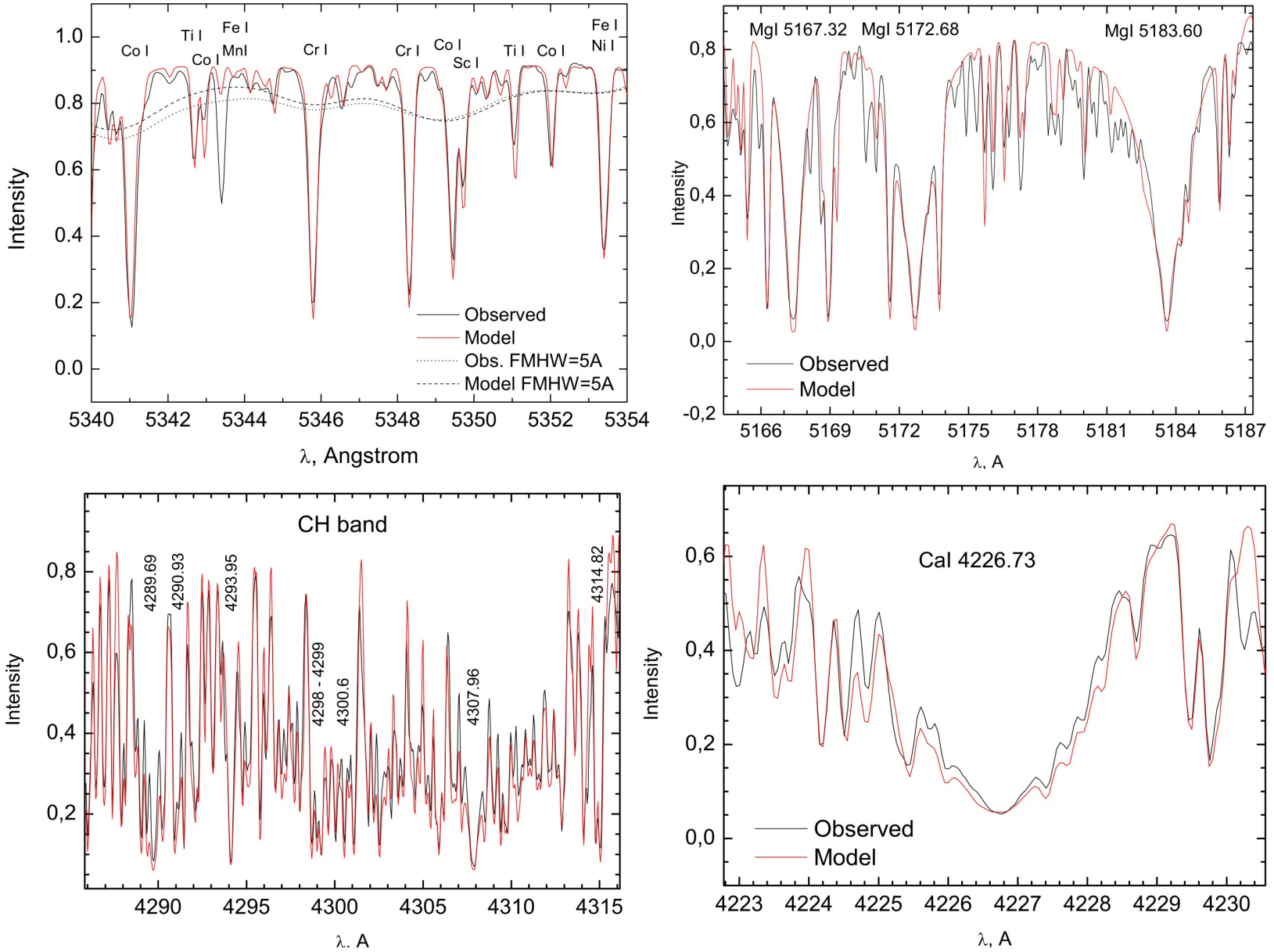


**Fig. A.1.** Comparison of the observed Arcturus spectrum from the ELODIE database and our calculated synthetic spectrum for a wavelength region including iron peak elements and for three wavelength regions corresponding to several prominent spectroscopic features (CH and MgH molecules, CaII H, K lines, CaI 4227 Å). The adopted parameters are from Ramírez & Prieto (2011).

We found t and Y by varying these parameters and calculating synthetic spectra until a good agreement between the observed and theoretical profiles of the Hgamma, Hdelta, and Hbeta lines was achieved. An indirect criterion for the correctness of the resulting parameters was simultaneous agreement between the observed and theoretical profiles for the CaI4226 A and CaII 3933, 3968 AA lines, with the same calcium abundance, confirming the correctness of the CaI/CaII ionization balance.
Decreasing the assumed age moves the isochrone's main-sequence turnoff point to higher temperatures. As a result, the contribution to the integrated light of the cluster of early main-sequence F dwarfs, whose Balmer lines have high intensities, increases. Thus, decreasing the age simultaneously strengthens the Doppler cores and wings of all H lines. Increasing the specific helium abundance Y has little influence on the shape of the isochrone for parts of the main sequence, subgiant, and red-giant phases, but increases the luminosities of hot HB stars. The H lines in the spectra of such stars are enhanced primarily in their Doppler cores, with pressure broadening be inginsignificant in their atmospheres. This means that increasing Y results primarily in large intensity increases in the central parts of the Balmer lines, while their wings become weaker. The largest increase in the calculated spectra is exhibited by Hb, and the smallest increase by Hdelta.

Comparison of the spectrum of NGC5286 (Schiavon et al., 2005) with the model spectra of [Fe/H]=-1.85 and different log(age), and helium content

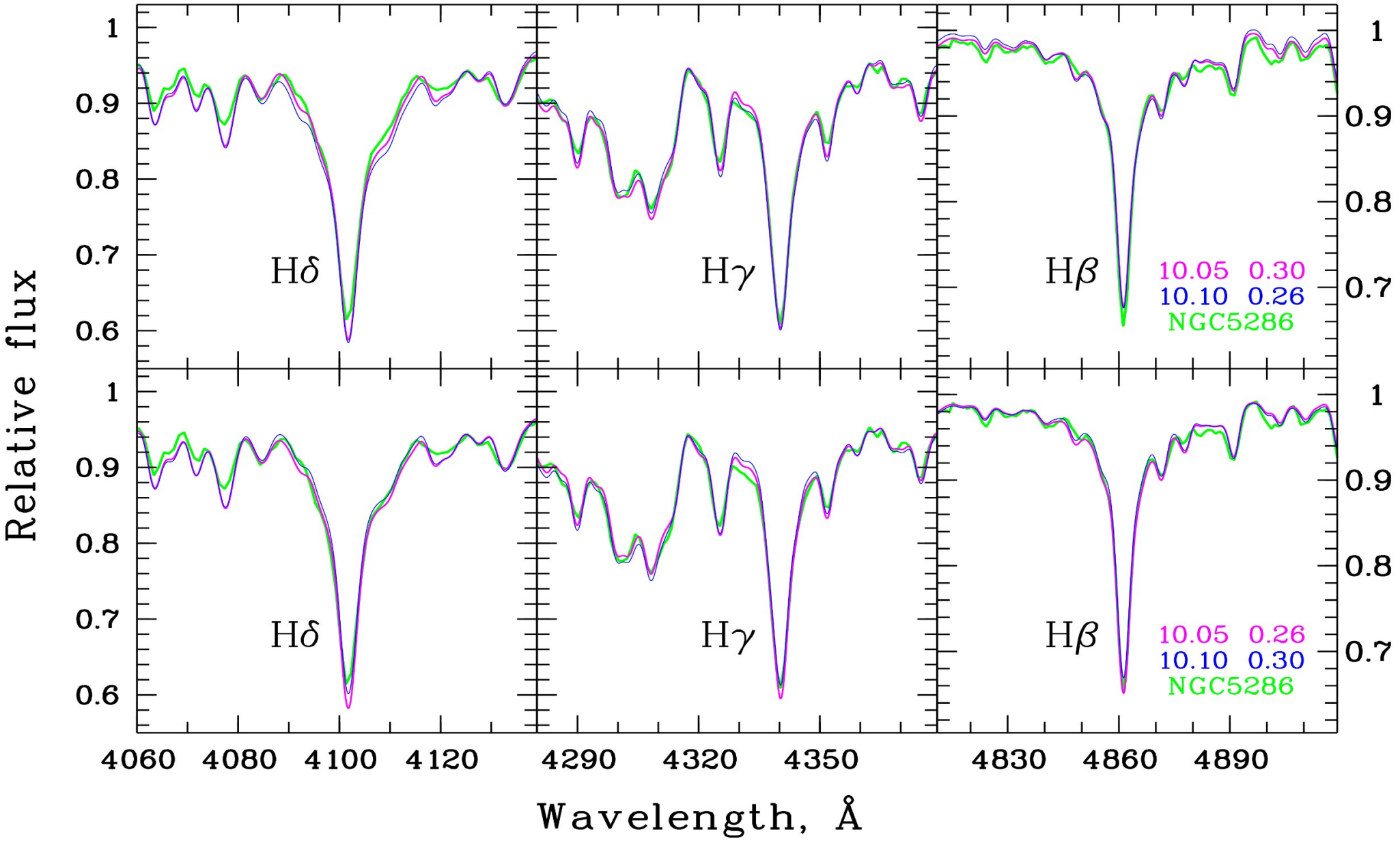

Comparison of the hydrogen lines in the spectra of 5 Galactic GCs from Schiavon et al. (2005)

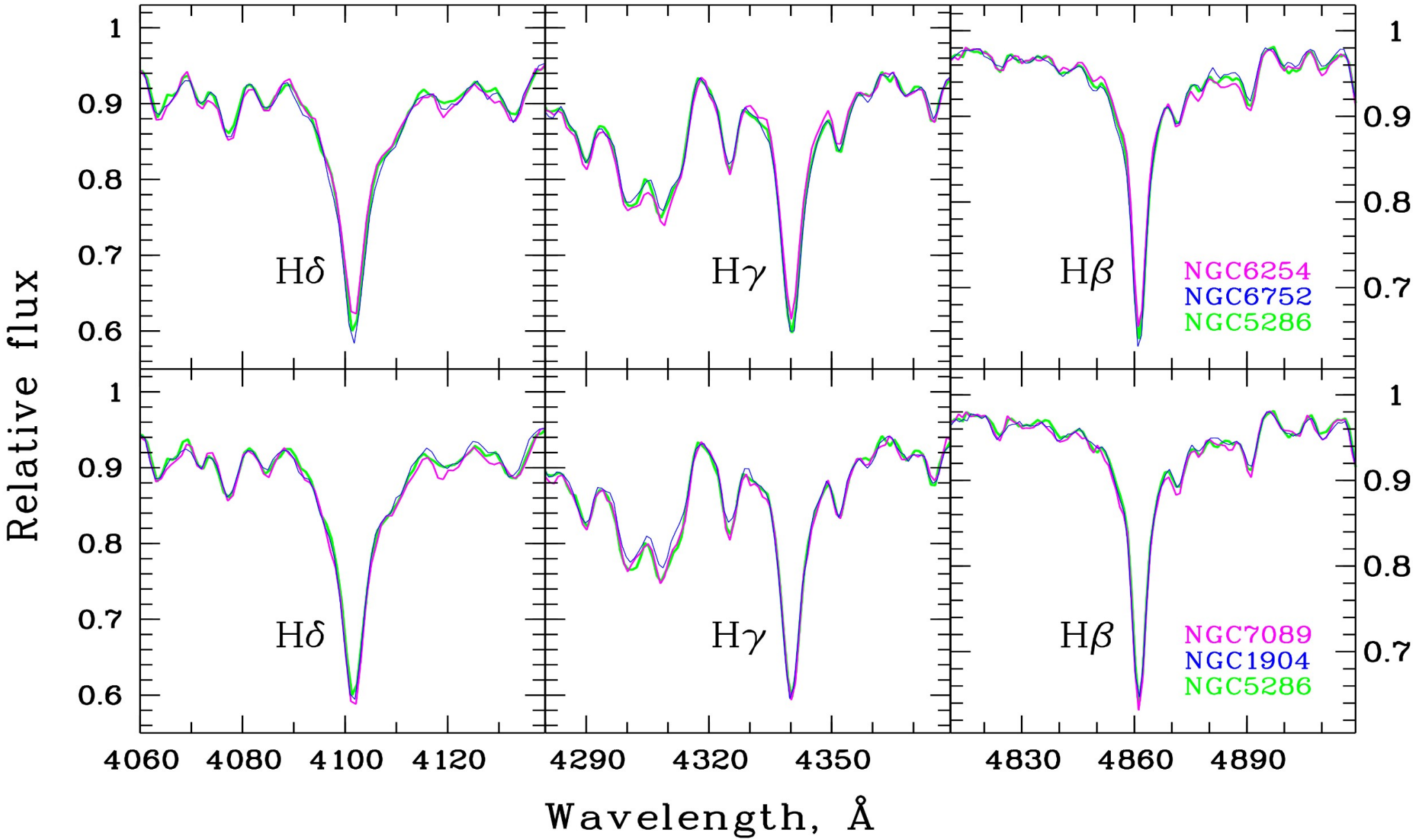

**Table 5.** Elemental abundances in dex from literature high-resolution spectroscopic studies of red giant stars in five Galactic GCs

| GC ID | [C/Fe] | [N/Fe] | [O/Fe] | [Na/Fe] | [Mg/Fe] | [Si/Fe] | [Ca/Fe] | [Ti/Fe] | [Cr/Fe] |
|---|---|---|---|---|---|---|---|---|---|
| NGC5286 (Mar15) | – | – | 0.44±0.22 | 0.34±0.22 | 0.55±0.22 | 0.40±0.22 | 0.31±0.22 | 0.33 ±0.22 | -0.05 ±0.22 |
| NGC1904 (R14) | – | – | 0.10±0.19 | 0.32±0.25 | 0.26±0.07 | 0.28±0.03 | 0.22±0.04 | 0.22±0.10 | -0.28±0.14 |
| NGC6752 (R14) | -0.45±0.37 | 0.93±0.63 | 0.26±0.25 | 0.32±0.26 | 0.38±0.15 | 0.47±0.19 | 0.31±0.09 | 0.20±0.11 | -0.13±0.12 |
| NGC7089 (R14-C, Y14 (r-only)) | -0.62±0.14 | – | 0.42±0.16 | 0.06±0.23 | 0.38±0.08 | 0.40±0.01 | 0.28±0.02 | 0.17±0.02 | -0.06±0.03 |
| NGC6254 (R14) | -0.77±0.37 | 1.01±0.45 | 0.23±0.24 | 0.17±0.27 | 0.44±0.13 | 0.28±0.07 | 0.33±0.11 | 0.26±0.12 | 0.01 ±0.15 |
| **NGC5286 (ours)** | **0.02±0.10** | **0.35±0.20** | **0.5±0.3** | **0.2±0.2** | **0.38±0.1** | **–** | **0.25±0.10** | **–** | **0.25±0.2** |
| **GC KKs3** | **-0.18±0.15** | **0.60±0.25** | **–** | **–** | **0.15±0.1** | **–** | **0.30±0.15** | **–** | **0.05±0.2** |
| **GC E269-66** | **-0.12±0.15** | **0.25±0.25** | **–** | **–** | **0.05±0.1** | **–** | **0.00±0.15** | **–** | **0.15±0.2** |

**Table 6.** Properties of the selected Galactic GCs. The data were taken from the catalogues by Kharchenko et al. (2013, K13) and Harris (2010, H10). We estimated approximately the ranges of $b$, $D_{GC}$, $V_r$, $\mu_l$, $\mu_b$, $X,Y$, for the Monoceros stream (MS) debris using the prograde motion model (pro1) by Penarrubia et al. (2005, P05) (Figures 8 and 11 in P05). The colums contain the following data: (2) Galactic longtitude and latitude $(l,b)$ from H10, (3) the range of $b$ at a given $l$ of each GC approximated using the MS model, (4) distance from the Sun (H10), (5) the range of distances from the Sun for the MS debris at a given $l$ of each GC, (6) heliocentric radial velocity from H10, (7) the range of heliocentric radial velocities for the model MS at a given $l$ of each GC, (8) proper motions in $l$ and $b$ from K13 for the GCs, (9) the range of $l$ and $b$ at a given $l$ of each GC for the model of MS, (10) Galactic distance components $X$, $Y$ and $Z$ in the Galactocentric coordinate system from H10, (11) the range of $Y$ at a given $X$ of each GC for the model of MS (we consider the nearest part of the stream (Fig.11, top panel in P05)), (12) Horizontal-branch ratio $(HBR = (B-R)/(B+V+R))$ from H10, (13) metallicity from H10, (14) King-model central concentration from H10, $c = log(r_t/r_c)$.

| GC ID | $l, b$ | $b^{MS}$ | $D_\odot$ | $D_\odot^{MS}$ | $V_r$ | $V_r^{MS}$ | $\mu_l*$, $\mu_b(\mu^{err})$ | $\mu_l*$, $\mu_b^{MS}$ | $X, \mathbf{Y}, Z$ | $\mathbf{Y}^{MS}$ | HBR | [Fe/H] |
|---|---|---|---|---|---|---|---|---|---|---|---|---|
| | [degr.] | [degr.] | [kpc] | [kpc] | [km/s] | [km/s] | [mas/yr] | [mas/yr] | [kpc] | [kpc] | | [dex] |
| | (2) | (3) | (4) | (5) | (6) | (7) | (8) | (9) | (10) | (11) | (12) | (13) |
| NGC1904 | 227.23,-29.35 | -40÷45 | 12.9 | 5÷40 | 205.8 | 0÷200 | -1.01, 0.30(0.43) | -7÷-1, -3÷7 | -15.6,**-8.3**,-6.3 | **-15÷23** | 0.89 | -1.60 |
| NGC5286 | 311.61, 10.57 | -25÷20 | 11.7 | 11÷40 | 57.4 | -50÷140 | -4.60, 0.21(0.83) | -7÷1, -2÷3 | -0.4,**-8.6**,2.1 | **-26÷10** | 0.80 | -1.69 |
| NGC6254 | 15.14, 23.08 | -27÷20 | 4.4 | 15÷50 | 75.2 | -120÷90 | -10.65,-0.75(0.36) | -6÷1, -2÷2 | -4.1,**1.1**,1.7 | **-26÷10** | 0.98 | -1.56 |
| NGC6752 | 336.49,-25.63 | -25÷25 | 4.0 | 15÷50 | -26.7 | -80÷150 | -5.19,-0.44(0.62) | -6÷1, -2÷2 | 4.7,**-1.4**,-1.7 | **-26÷10** | 1.00 | -1.54 |
| NGC7089 | 53.37,-35.77 | -30÷25 | 11.5 | 12÷40 | -5.3 | -200÷70 | -0.05,-6.24(0.42) | -6÷1, -2÷2 | -2.4,**7.5**,-6.7 | **10÷30** | 0.96 | -1.65 |

- Massive Galactic GCs with extended horizontal branches (EHBs) and multiple stellar populations show spatial distribution, kinematic and structural properties distinct to that of other Galactic GCs (Lee et al. 2007). They might be formed in old Galactic building blocks and accreted during assembling process of the halo. Galactic GCs are divided in two groups - 1) old objects with almost the same age and no age-metallicity relation (AMR) and 2) younger clusters following the AMR of the Sgr dSph (Marin-Franch et al., 2009, M-F09). Five selected GCs with similar spectra **(NGC6254, NGC7089, NGC5286, NGC6752 and NGC1904)** have metallicity z = 0.0004, helium content Y = 0.30 and log(Age) = 10.10, according to our analysis. Chemical composition of the GCs is very similar according to our analysis and high-resolution spectroscopic studies. All these GCs were classified as old halo objects by M-F09. At the same time, they correspond well the age-metallicity relation of the Sgr dSph and CMa dwarf galaxies (Forbes & Bridges, 2010).
- A mean metallicity of the group is [Fe/H]=-1.6 dex. They have extended blue horizontal branches and similar half-light radii Rh~2.7 pc. Their absolute magnitudes in the V-band are in the range: from -7.7 (NGC6752) to -9.0 (NGC7089). Multiple stellar population were discovered in NGC5286 (Marino et al., 2015),NGC7089 (Young et al., 2014), NGC6752 (Dotter et al., 2015).

- Three of the five GCs were accociated with the Sgr and Monoceros stream in the literature (Bellazzini et al. 2003, Penarrubia et al. (2005): NGC1904 (MS), NGC5286 (MS),NGC7089 (Sgr. Stream).
  Table 6 shows the comparison of the properties of these GCs with the corresponding parameters for the the prograde motion model (pro1) of the Monoceros Stream by Penarrubia et al. (2005, their Figures 8 and 11).
  It is seen that all the properties of NGC6254, NGC6752 and NGC7089, except for a few, are consistent with that of the MS. The galactocentric distances of NGC6254 and NGC6752 look too small.
  The proper motions of NGC6254 and NGC7089 are large.
  Note, however, that NGC6254 and NGC6752 are fainter then the other objects and locate closer to the Galactic plane. If the objects experienced interaction with the Galactic disk , their orbits might have been changed.